

Bergman, Aza-Bergman, and Protonated Aza-Bergman Cyclizations and Intermediate 2,5-Arynes: Chemistry and Challenges to Computation

Christopher J. Cramer

Contribution from the Department of Chemistry and Supercomputer Institute, 207 Pleasant St. SE, Minneapolis, Minnesota 55455-0431

Received February 27, 1998

Abstract: Reaction coordinates are computed for the Bergman cyclizations of hex-3-en-1,5-diyne and neutral and protonated 3-azahex-3-en-1,5-diyne at various levels of correlated electronic structure theory, as are singlet–triplet splittings for intermediate arynes. To be effective in low-symmetry situations showing high degrees of biradical character, CCSD(T) calculations benefit from use of Brueckner orbitals. Replacement of a CH fragment by N is predicted to increase the stability of the aryne relative to the iminediyne, and to increase drastically the stability of the isomeric enynenitrile. The barrier for retro-aza-Bergman cyclization of 2,5-pyridyne to pent-3-en-1-yne nitrile is predicted to be only 0.9 kcal/mol, which, combined with a predicted singlet–triplet splitting of –11.6 kcal/mol, suggests that 2,5-pyridynes are poor hydrogen atom abstracting agents. Protonation of nitrogen decreases the singlet–triplet splitting and raises the barrier to retro-aza-Bergman cyclization such that protonated 2,5-pyridynes may be expected to show reactivities similar to all-carbon analogues.

1. Introduction

The Bergman cyclization converts a 3-en-1,5-diyne to a 1,4-didehydroaryne;^{1,2} the simplest example, then, is the conversion of hex-3-ene-1,5-diyne to 1,4- (or *para*-) benzyne. In organic chemistry, arynes have long been known to be reactive intermediates in various chemical transformations.^{3–6} Renewed interest in 1,4-arynes derives from their cytotoxic activity when formed *in vivo* as reactive intermediates from a member of the so-called enediyne class of antibiotics,^{7–10} e.g., calicheamicin.⁷ An enediyne antibiotic selectively cyclizes when complexed in the minor groove of double-stranded DNA, and the resulting 1,4-aryne is positioned in such a way that it abstracts two hydrogen atoms, one from each strand of the DNA, to form a much more thermodynamically stable arene.¹¹ The damaged DNA suffers cleavage along both strands, and this damage can ultimately lead to cell death.

Arynes, and more recently the Bergman reaction, have also been of particular interest to theorists,^{3,12–25} in part because they pose unique challenges to computational technology. As Chen

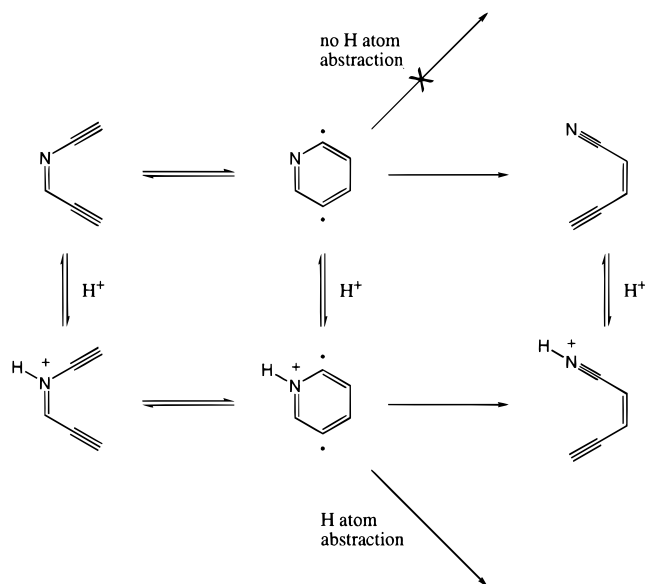
has emphasized,^{26–29} the reactivity of the aryne antitumor agents derives from the small separation between their singlet and triplet states; i.e., they have high degrees of biradical character. Such a situation typically involves a near degeneracy between two frontier orbitals, and single-determinant levels of theory (like Hartree–Fock) are often inadequate for the treatment of such systems. Multireference techniques (e.g., MCSCF) can account for nondynamical correlation,³⁰ but in order to calculate state energy splittings to chemically useful levels of accuracy, one typically requires an accounting for dynamical correlation effects as well,³¹ and such levels of theory can be particularly taxing of computational resources for molecules of even moderate size.

Returning to the issue of biological activity, the antitumor activity of the enediyne antibiotics has up to now been mitigated by their high cytotoxicity to normal cells.¹⁰ Recently, as

- (1) Jones, R. R.; Bergman, R. G. *J. Am. Chem. Soc.* **1972**, *94*, 660.
- (2) Bergman, R. G. *Acc. Chem. Res.* **1973**, *6*, 25.
- (3) Hoffmann, R. W. *Dehydrobenzene and Cycloalkynes*; Academic Press: New York, 1967.
- (4) Gilchrist, T. L.; Rees, C. W. *Carbenes, Nitrenes, and Arynes*; Nelson: London, 1969.
- (5) Wentrup, C. *Reactive Molecules*; Wiley: New York, 1984; p 288.
- (6) Levin, R. H. In *Reactive Intermediates*; Jones, M., Moss, R., Eds.; Wiley: New York, 1985; Vol. 3, p 1.
- (7) Lee, M. D.; Dunne, T. S.; Chang, C. C.; Ellestad, G. A.; Siegel, M. M.; Morton, G. O.; McGahren, W. J.; Borders, D. B. *J. Am. Chem. Soc.* **1987**, *109*, 3466.
- (8) Nicolaou, K. C.; Smith, A. L. *Acc. Chem. Res.* **1992**, *25*, 497.
- (9) Gleiter, R.; Kratz, D. *Angew. Chem.* **1993**, *105*, 884.
- (10) *Enediyne Antibiotics as Antitumor Agents*; Borders, D. B., Doyle, T. W., Eds.; Marcel Dekker: New York, 1995.
- (11) Nicolaou, K. C.; Dai, W.-M. *Angew. Chem.* **1991**, *103*, 1453.
- (12) Scheiner, A. C.; Schaefer, H. F., III; Liu, B. *J. Am. Chem. Soc.* **1989**, *111*, 3118.
- (13) Nicolaidis, A.; Borden, W. T. *J. Am. Chem. Soc.* **1993**, *115*, 11951.

- (14) Wierschke, S. G.; Nash, J. J.; Squires, R. R. *J. Am. Chem. Soc.* **1993**, *115*, 11958.
- (15) Kraka, E.; Cremer, D. *J. Am. Chem. Soc.* **1994**, *116*, 4929.
- (16) Lindh, R.; Persson, B. J. *J. Am. Chem. Soc.* **1994**, *116*, 4963.
- (17) Lindh, R.; Lee, T. J.; Bernhardsson, A.; Persson, B. J.; Karlström, G. *J. Am. Chem. Soc.* **1995**, *117*, 7186.
- (18) Cramer, C. J.; Nash, J. J.; Squires, R. R. *Chem. Phys. Lett.* **1997**, *277*, 311.
- (19) Cramer, C. J.; Squires, R. R. *J. Phys. Chem. A* **1997**, *101*, 9191.
- (20) Kraka, E.; Cremer, D.; Bucher, G.; Wandel, H.; Sander, W. *Chem. Phys. Lett.* **1997**, *268*, 313.
- (21) Lindh, R.; Ryde, U.; Schütz, M. *Theor. Chem. Acc.* **1997**, *97*, 203.
- (22) Schreiner, P. R. *J. Chem. Soc., Chem. Commun.* **1998**, 483.
- (23) Chen, W.-C.; Chang, N.-y.; Yu, C.-h. *J. Phys. Chem. A* **1998**, *102*, 2584.
- (24) Cramer, C. J.; Debbert, S. *Chem. Phys. Lett.* **1998**, *287*, 320.
- (25) Schreiner, P. R. *J. Am. Chem. Soc.* **1998**, *120*, 4184.
- (26) Logan, C. F.; Chen, P. *J. Am. Chem. Soc.* **1996**, *118*, 2113.
- (27) Schottelius, M. J.; Chen, P. *J. Am. Chem. Soc.* **1996**, *118*, 4896.
- (28) Chen, P. *Angew. Chem.* **1996**, *108*, 1584.
- (29) Hoffner, J.; Schottelius, M. J.; Feichtinger, D.; Chen, P. *J. Am. Chem. Soc.* **1998**, *120*, 376.
- (30) Roos, B. O.; Taylor, P. R.; Siegbahn, P. E. M. *Chem. Phys.* **1980**, *48*, 157.
- (31) Borden, W. T.; Davidson, E. R. *Acc. Chem. Res.* **1996**, *29*, 67.

Scheme 1



illustrated in Scheme 1, Chen has made the creative suggestion that an enediyne with one carbon atom replaced by nitrogen (i.e., an azaenediyne) might be used to overcome this difficulty.²⁸ Normal and tumor cells can be differentiated by their pH, with the tumor cells being up to 1.7 p*K*_a units lower in pH under certain physiological conditions.³² By taking advantage of this difference to generate an aza-aryne in either a protonated or unprotonated state depending on the nature of the cell, one might be able to target the DNA-cleaving ability if the protonated aza-aryne is more reactive as a hydrogen-atom abstracting agent than the unprotonated form. Hoffner et al.²⁹ subsequently reported kinetic and trapping studies of neutral and protonated substituted 2,5-didehydropyridines; they observed no hydrogen abstraction reactivity for the neutral case (an observation also made previously by David and Kerwin³³), but measurable levels of such activity at pH values where a substantial fraction of the reacting molecules would be expected to be protonated. These results appear to be quite promising, then, in terms of viability for further drug design efforts.

In addition to their experimental results, Hoffner et al.²⁹ carried out *ab initio* calculations for the reaction thermochemistry and singlet–triplet splittings of the all-carbon and aza-substituted hex-3-ene-1,5-diyne prototypes. These studies chose rather unusual active spaces for CASSCF calculations and accounted for dynamical correlation with orthogonal valence bond second-order perturbation theory³⁴ (OVBP2), a level which has seen little testing in the literature and would in general be expected³⁵ to be inferior to more modern implementations of multireference perturbation theory. For the all-carbon case, where experimental results are available for the cyclization thermochemistry³⁶ and singlet–triplet splitting,³⁷ this led to fairly substantial errors: a calculated barrier height too high by 13 kcal (all energies in this article are molar), an endothermicity in error by 9 kcal, and a state energy splitting in error by 3 kcal.

(32) von Ardenne, M. *Adv. Pharmacol. Chemot. (San Diego)* **1972**, *10*, 339.

(33) David, W. M.; Kerwin, S. M. *J. Am. Chem. Soc.* **1997**, *119*, 1464.

(34) McDouall, J. J.; Peasley, K.; Robb, M. A. *Chem. Phys. Lett.* **1988**, *148*, 183.

(35) Andersson, K.; Malmqvist, P.-Å.; Roos, B. O. *J. Chem. Phys.* **1992**, *96*, 1218.

(36) Roth, W. R.; Hopf, H.; Horn, C. *Chem. Ber.* **1994**, *127*, 1765.

(37) Wenthold, P. G.; Squires, R. R.; Lineberger, W. C. *J. Am. Chem. Soc.* **1998**, *120*, 5279–5290.

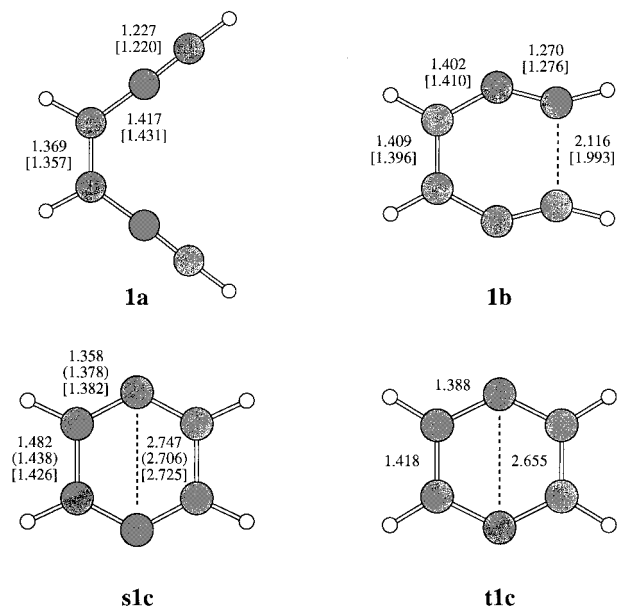


Figure 1. Stationary points along the all-carbon Bergman cyclization reaction coordinate. Heavy atom bond lengths (Å) are indicated from BPW91/cc-pVDZ, (broken spin-symmetry BPW91/cc-pVDZ), and [CCSD(T)/6-31G**] calculations.

In this paper, I apply a variety of different levels of theory, including CASPT2 multireference second-order perturbation theory, density functional theory (DFT), and coupled-cluster theories including perturbative estimations of the effects of triple excitations with both Hartree–Fock and Brueckner orbitals, CCSD(T) and BCCD(T), respectively, to provide more quantitative values for the Bergman, aza-Bergman, and protonated aza-Bergman cycloadditions. For the all-carbon case, these results are compared against experiment and prior high-level computations. The 2,5-didehydropyridinium singlet requires the use of Brueckner orbitals to overcome instability otherwise inherent in the CCSD(T) approach, a feature likely to prove true in general for low-symmetry biradicals having narrow HOMO–LUMO gaps; discussion of technical aspects of the theory is provided.

2. Computational Methods

Molecular geometries for all species were optimized at the density functional level of theory with the cc-pVDZ basis set³⁸ (Figures 1–3). For **s1c**, **s2c**, and **s3c**, both restricted and broken-spin-symmetry optimizations were carried out (the broken-symmetry energy of **s2c** was only 0.4 kcal lower than the restricted energy and reoptimization has no noticeable impact on the geometry). MCSCF calculations were of the complete active space (CAS) variety. For arynes **1c** and **3c**, 8-electron/8-orbital active spaces comprised of the 6 π orbitals and the 2 nonbonding σ orbitals were used. For aryne **2c**, the analogous space was augmented with the nitrogen lone pair to create a (10,9) active space. For Bergman stationary points **1a**, **1b**, **3a**, **3b**, **3d**, and **3e**, (10,10) active spaces were comprised of all of the π orbitals. For stationary points **2a**, **2b**, **2d**, and **2e**, these active spaces were expanded to (12,11) by inclusion of the nitrogen lone pair.

DFT calculations employed the gradient-corrected functionals of Becke³⁹ and Perdew et al.⁴⁰ (BPW91). All DFT geometries were confirmed as local minima by computation of analytic vibrational frequencies, which were also used to compute zero-point vibrational energies (ZPVE) and thermal enthalpy contributions ($H_{298} - H_0$). Total spin expectation values for Slater determinants formed from the

(38) Dunning, T. H. *J. Chem. Phys.* **1989**, *90*, 1007.

(39) Becke, A. D. *Phys. Rev. A* **1988**, *38*, 3098.

(40) Perdew, J. P.; Burke, K.; Wang, Y. *Phys. Rev. B* **1996**, *54*, 6533.

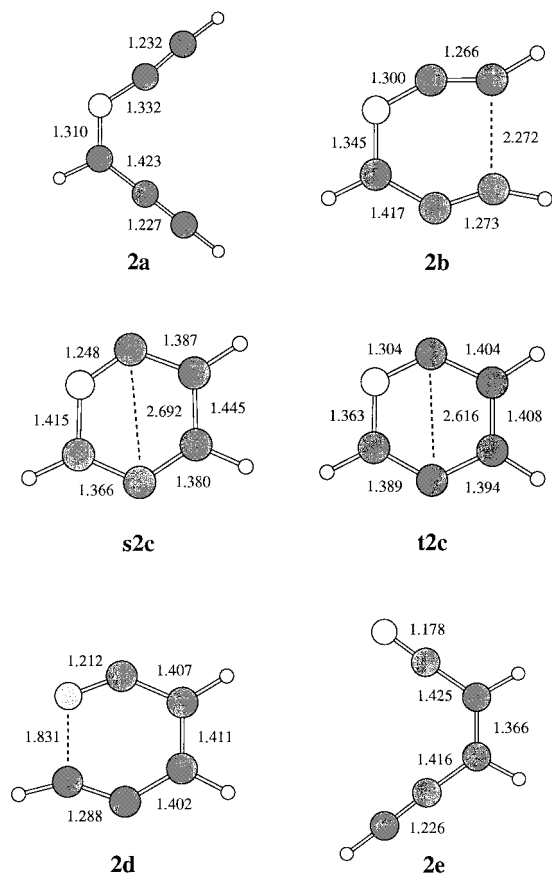


Figure 2. Stationary points along the aza-Bergman cyclization reaction coordinate. Heavy atom bond lengths (Å) are indicated from BPW91/cc-pVDZ calculations.

optimized (unrestricted) Kohn–Sham orbitals did not exceed 2.03 for the triplets and were on the order of 0.8 for the broken-spin-symmetry singlets.

To improve the molecular orbital calculations, dynamic electron correlation with the CAS reference was accounted for at the CASPT2 level.^{41–43} Some caution must be applied in interpreting the CASPT2 results since this level of theory is known to suffer from a systematic error proportional to the number of unpaired electrons,⁴² and that number changes along the Bergman reaction coordinate. CCSD(T)^{44–47} and BCCD(T)⁴⁸ calculations with the Hartree–Fock reference wave function were also carried out (instead of HF orbitals, BCCD(T) uses Brueckner orbitals, which eliminate contributions from single excitations in the CC ansatz). All correlated calculations employed the cc-pVDZ basis set; CCSD/cc-pVTZ energies were also determined for each structure to evaluate the effects of basis set incompleteness. When reported in the text,

$$\text{composite E} = \text{BCCD(T)/cc-pVDZ} + [\text{CCSD/cc-pVTZ} - \text{CCSD/cc-pVDZ}] \quad (1)$$

Note that instabilities discussed below for the CCSD(T) level were

(41) Andersson, K.; Malmqvist, P.-Å.; Roos, B. O.; Sadlej, A. J.; Wolinski, K. *J. Phys. Chem.* **1990**, *94*, 5483.

(42) Andersson, K.; Roos, B. O. *Int. J. Quantum Chem.* **1993**, *45*, 591.

(43) Andersson, K.; Blomberg, M. R. A.; Fülscher, M. P.; Karlström, G.; Kellö, V.; Lindh, R.; Malmqvist, P.-Å.; Noga, J.; Olsen, J.; Roos, B. O.; Sadlej, A. J.; Siegbahn, P. E. M.; Urban, M.; Widmark, P.-O. *MOLCAS-3*; University of Lund: Sweden, 1994.

(44) Cizek, J. *Adv. Chem. Phys.* **1969**, *14*, 35.

(45) Purvis, G. D.; Bartlett, R. J. *J. Chem. Phys.* **1982**, *76*, 1910.

(46) Gauss, J.; Cremer, C. *Chem. Phys. Lett.* **1988**, *150*, 280.

(47) Raghavachari, K.; Trucks, G. W.; Pople, J. A.; Head-Gordon, M. *Chem. Phys. Lett.* **1989**, *157*, 479.

(48) Handy, N.; Pople, J. A.; Head-Gordon, M.; Raghavachari, K.; Trucks, G. W. *Chem. Phys. Lett.* **1989**, *164*, 185.

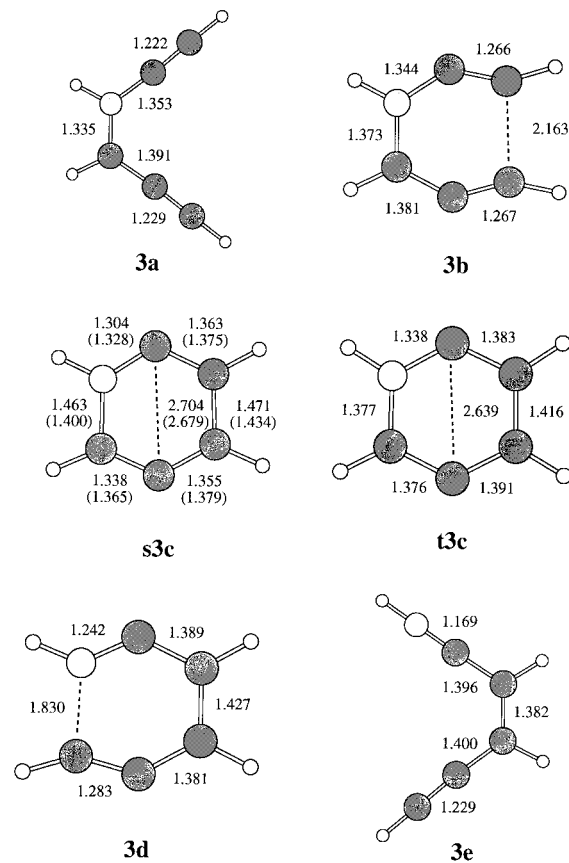


Figure 3. Stationary points along the N-protonated aza-Bergman cyclization reaction coordinate. Heavy atom bond lengths (Å) are indicated from BPW91/cc-pVDZ and (broken spin-symmetry BPW91/cc-pVDZ) calculations.

not a problem at the CCSD level, making this level the most efficient choice for evaluating basis set completeness.

Isotropic hyperfine coupling constants (hfs) were calculated as⁴⁹

$$a_X = (4\pi/3) \langle S_z \rangle^{-1} g g_X \beta \beta_X \rho(X) \quad (2)$$

where g is the electronic g factor, β is the Bohr magneton, g_X and β_X are the corresponding values for nucleus X , and $\rho(X)$ is the Fermi contact integral

$$\rho(X) = \sum_{\mu\nu} P_{\mu\nu}^{\alpha-\beta} \phi_\mu(\mathbf{R}_X) \phi_\nu(\mathbf{R}_X) \quad (3)$$

where $\mathbf{P}^{\alpha-\beta}$ is the BPW91/cc-pVDZ one-electron spin density matrix, and evaluation of the overlap between basis functions ϕ_μ and ϕ_ν is only at the nuclear position, \mathbf{R}_X .

Electrostatic components of the aqueous solvation free energies for the various cationic structures were calculated at the BPW91 level with the MIDI! basis set⁵⁰ and generalized Born theory⁵¹ with CM2 charge⁵² and SM5.42R solvation⁵³ parameters. For water, the dielectric constant was taken to be 78.3.

(49) Lim, M. H.; Worthington, S. E.; Dulles, F. J.; Cramer, C. J. In *Density-Functional Methods in Chemistry*; Laird, B. B., Ross, R. B., Ziegler, T., Eds.; American Chemical Society: Washington, DC, 1996; p 402.

(50) Easton, R. E.; Giesen, D. J.; Welch, A.; Cramer, C. J.; Truhlar, D. G. *Theor. Chim. Acta* **1996**, *93*, 281.

(51) Cramer, C. J.; Truhlar, D. G. In *Solvent Effects and Chemical Reactivity*; Tapia, O., Bertrán, J., Eds.; Kluwer: Dordrecht, 1996; p 1.

(52) Li, J.; Zhu, T.; Cramer, C. J.; Truhlar, D. G. *J. Phys. Chem. A* **1998**, *102*, 1820.

(53) Zhu, T.; Li, J.; Hawkins, G. D.; Cramer, C. J.; Truhlar, D. G. *J. Chem. Phys.* Submitted for publication.

All CAS and DFT calculations were carried out with the MOLCAS⁴³ and Gaussian 94⁵⁴ electronic structure program suites, respectively.

3. Results

Geometries. The structures for all stationary points along the various Bergman cyclization pathways (as well as for the aryne triplets) are provided in Figures 1–3. Structures **a** are enediynes with the nitrogen atom (if present) at the 3-position and structures **b** are transition states connecting enediynes **a** to (singlet, indicated by a preceding **s**) arynes **c**. Retro-Bergman reaction to break the C–N bond is possible for compounds **2** and **3**; structures **d** are the transition states for this process, and structures **e** are the enynenitriles produced from retrocyclization. Imaginary frequencies for the various transition states are 423i (**1b**), 360i (**2b**), 456i (**2d**), 399i (**3b**), and 441i (**3d**). Triplet arynes **c** are indicated by a preceding **t**. Heavy atom bond lengths are listed in the figures, and optimized Cartesian coordinates are provided as Supporting Information. Figure 1 also includes bond lengths calculated at the CCSD(T)/6-31G** level as reported by Kraka and Cremer.^{15,55}

For singlets **s1c** and **s3c**, the restricted Kohn–Sham determinant is observed to be unstable to spin-symmetry breaking. Unrestricted broken-spin-symmetry DFT (BS–UDFT) energies are about 6 kcal lower than restricted energies, and reoptimization at the unrestricted level leads to fairly substantial changes in geometry for each case; bond length data are available in Figures 1 and 3. Such symmetry breaking leads to a mixing of spin states but is well-known^{56,57} to be efficacious in better describing inorganic systems where localization of spin occurs at two (or more) metal sites, for instance. Note that the *geometries* do not lose symmetry, remaining D_{2h} and C_s , respectively—only spin symmetry is broken. In favorable instances, the BS–UDFT energy can be analyzed to obtain energies for the different states contributing to the final density, including potentially states that cannot be described by a single determinant.^{49,58–60} For **s1c** and **s3c**, however, the weights of the contributions from various singlet and triplet (and higher spin) states are not easily determined, so interpreting the energy directly may be somewhat risky. Nevertheless, the BS–UDFT geometries are definitely improved over the restricted DFT geometries, as judged by single-point calculations at other high-quality levels of theory (*vide infra*). Kraka et al. have noted

(54) Frisch, M. J.; Trucks, G. W.; Schlegel, H. B.; Gill, P. M. W.; Johnson, B. G.; Robb, M. A.; Cheeseman, J. R.; Keith, T.; Petersson, G. A.; Montgomery, J. A.; Raghavachari, K.; Al-Laham, M. A.; Zakrzewski, V. G.; Ortiz, J. V.; Foresman, J. B.; Cioslowski, J.; Stefanov, B. B.; Nanayakkara, A.; Challacombe, M.; Peng, C. Y.; Ayala, P. Y.; Chen, W.; Wong, M. W.; Andres, J. L.; Replogle, E. S.; Gomperts, R.; Martin, R. L.; Fox, D. J.; Binkley, J. S.; Defrees, D. J.; Baker, J.; Stewart, J. P.; Head-Gordon, M.; Gonzalez, C.; Pople, J. A. *Gaussian 94 RevD.1*; Gaussian Inc.: Pittsburgh, PA, 1995.

(55) The CCSD(T) calculations of Kraka and Cremer included excitations from the heavy atom core orbitals. The energies listed as CCSD(T)/6-31G** in Table 3, however, were computed with frozen core orbitals, and thus the absolute energies differ from those reported by Kraka and Cremer in ref 15. The effect on the relative energies of including core excitations is very small: the energy of **1a** drops by 0.4 kcal/mol relative to **1b** and **s1c**. One would further expect including or freezing the core orbitals to have no noticeable impact on the geometries. Note that the published CCSD(T)/6-31G** geometry for **1a** lists the innermost CCC valence angle as 120.6°, but the correct value is 124.1° (Kraka, E.; Cremer, D. Personal communication). All computations in Table 3 used the correct structure.

(56) Noodleman, L.; Case, D. A. *Adv. Inorg. Chem.* **1992**, *38*, 423.

(57) Lovell, T.; McGrady, J. E.; Stranger, R.; Macgregor, S. *Inorg. Chem.* **1996**, *35*, 3079.

(58) Slater, J. C. *Adv. Quantum Chem.* **1972**, *6*, 1.

(59) Ziegler, T.; Rauk, A.; Baerends, E. J. *Theor. Chim. Acta* **1977**, *43*, 261.

(60) Cramer, C. J.; Dulles, F. J.; Giesen, D. J.; Almlöf, J. *Chem. Phys. Lett.* **1995**, *245*, 165.

this previously for *m*-benzynes.²⁰ Structure **s2c** teeters on the edge of instability: a BS–UDFT calculation lowers the absolute energy by just 0.4 kcal and reoptimization of the geometry leads to chemically inconsequential changes (the energy drops another 0.01 kcal and all bond length changes are less than 0.0004 Å). Thus, all data in this paper for **s2c** are from the restricted DFT formalism and geometry. All other stationary points, including transition state structures for **1**, **2**, and **3** are stable to spin-symmetry breaking, consistent with their much smaller degree of multireference character (*vide infra*).

Cyclization Thermochemistry. Table 1 provides relative 298 K enthalpies for the various stationary points along the Bergman and aza-Bergman cyclization reaction coordinates for **1–3** as calculated at several levels of theory. Precedent suggests that all of these levels should be capable of handling moderate to large degrees of multireference character in molecular wave functions. Also included are the OVBPT2 results of Hoffner et al.²⁹ and, for the all-carbon case **1**, the experimental results of Roth et al.³⁶ (note that an independent measurement of $\Delta H_{f,298}^{\circ}$ for *p*-benzynes in the gas phase has been reported by Wenthold and Squires⁶¹ that, when combined with the known $\Delta H_{f,298}^{\circ}$ of hex-3-ene-1,5-diyne,⁶² provides a reaction endothermicity of 8.3 ± 2.9 kcal for the Bergman reaction, in excellent agreement with the Roth solution results³⁶).

Singlet–triplet splittings were also calculated for the **1–3** aryne spin isomers **s** and **t** at these same levels. These results (H_0) are compiled in Table 2, along with the predictions of Hoffner et al.²⁹ at the OVBPT2 level and the experimental results of Wenthold et al.³⁷ for **1**.

4. Discussion

I begin this section by examining specific technical issues associated with the various computational methods. The implications of the calculations and best estimates for the barrier heights and singlet–triplet splittings in systems **2** and **3** are discussed thereafter.

Theoretical Methods. The success of DFT in the prediction of molecular (and electronic) structures for ordinary closed-shell organic molecules has become an accepted axiom of computational chemistry. For certain more complicated species, however—even systems well represented by a single determinant description—rather severe deficiencies have been noted, e.g., partially bonded systems,⁶³ certain phosphoranyl radicals,⁴⁹ and certain radical ions.⁶⁴ Another open question is the limitations of DFT when applied to systems having some degree of multireference character. Many papers have appeared applying standard DFT methods to carbenes and analogous systems including hypovalent second- or third-row atoms, and results have in general been very good for such properties as molecular geometries, singlet–triplet splittings, etc.^{49,60,65–85} Thus, by construction of the functional, DFT is capable of accurately representing systems that at the molecular orbital level

(61) Wenthold, P.; Squires, R. R. *J. Am. Chem. Soc.* **1994**, *116*, 6401.
(62) Roth, W. R.; Adamczak, O.; Breuckmann, R.; Lennartz, H.-W.; Boese, R. *Chem. Ber.* **1991**, *124*, 2499.

(63) Ruiz, E.; Salahub, D.; Vela, A. *J. Am. Chem. Soc.* **1995**, *117*, 1141.
(64) Bally, T.; Sastry, G. N. *J. Phys. Chem.* **1997**, *101*, 7923.

(65) Jones, R. O. *J. Chem. Phys.* **1985**, *82*, 325.
(66) Radzio, E.; Salahub, D. R. *Int. J. Quantum Chem.* **1986**, *29*, 241.
(67) *Density Functional Methods in Chemistry*; Labanowski, J., Andzelm, J., Eds.; Springer-Verlag: New York, 1991.

(68) Gutsev, G. L.; Ziegler, T. *J. Phys. Chem.* **1991**, *95*, 7220.
(69) Murray, C. W.; Handy, N. C.; Amos, R. D. *J. Chem. Phys.* **1993**, *98*, 7145.

(70) Russo, N.; Sicilia, E.; Toscano, M. *Chem. Phys. Lett.* **1993**, *213*, 245.

(71) Jacobsen, H.; Ziegler, T. *J. Am. Chem. Soc.* **1994**, *116*, 3667.

Table 1. Relative Enthalpies (H_{298} , kcal/mol) of Stationary Points along Isoelectronic Bergman Cyclization Pathways^a

compd	level of theory ^b					
		a	b	c(s)	d	e
1, Z = CH	BPW91	0.0	22.0	0.9 (7.0)		
	CASPT2	0.0	21.7	-2.6 (-1.3)		
	CCSD(T)	0.0	25.6	4.8 (6.9)		
	BCCD(T)	0.0	25.6	4.8 (7.0)		
	composite E ^d	0.0	27.7	11.0 (12.1)		
	OVBP2 ^e	0.0	33.7	0.1		
2, Z = N	BPW91	0.0	14.5	-14.5	-8.8	-38.1
	CASPT2	0.0	16.3	-19.8	-11.0	-43.6
	CCSD(T)	0.0	17.4	-10.7	-8.0	-45.1
	BCCD(T)	0.0	17.5	-9.7	-7.9	-45.0
	composite E ^d	0.0	19.4	-5.3	-4.4	-42.8
	OVBP2 ^e	0.0	26.8	-11.0	-1.5	-43.8
3, Z = NH ⁺	BPW91	0.0	18.3	-6.9 (-0.2)	3.2	-29.3
	CASPT2	0.0	18.2	-15.1 (-13.2)	0.4	-30.2
	CCSD(T)	0.0	19.9	-30.6 (-10.3)	6.5	-29.9
	BCCD(T)	0.0	19.9	-7.0 (-3.9)	6.4	-29.9
	composite E ^d	0.0	21.6	-1.4 (0.6)	9.3	-29.8
	OVBP2 ^e	0.0	29.1	-11.8	16.8	-28.7

^a Geometries and thermal rovibrational contributions from the BPW91/cc-pVDZ level. ^b See Methods section for details on basis sets and CASPT2 active spaces. ^c For **1** and **3**, results are for broken spin symmetry geometries; restricted geometry results are in parentheses (for BPW91 results, a restricted determinant was employed for the restricted geometry). ^d Equation 1. ^e Reference 29 with BPW91/cc-pVDZ thermal contributions. ^f Reference 36.

of theory would otherwise require accounting for dynamical and/or nondynamical correlation effects. However, there are limitations in the amount of nondynamical correlation (i.e., multireference character) that can be accounted for within that formalism. By analysis of the ring-opening of methylenecyclopropane to make trimethylenemethane (a non-Kekulé diradical that, in the absence of Jahn–Teller distortion, requires a 50:50 two-configuration description for an adequate singlet wave function), Cramer and Smith⁸⁶ found various functionals to lose their predictive utility at a point where the two dominant configurations in the MCSCF wave function came into a ratio of about 75:25.

(72) Arduengo, A. J.; Bock, H.; Chen, H.; Denk, M.; Dixon, D. A.; Green, J. C.; Herrmann, W. A.; Jones, N. L.; Wagner, M.; West, R. *J. Am. Chem. Soc.* **1994**, *116*, 6641.

(73) Arduengo, A. J.; Rasika Dias, H. V.; Dixon, D. A.; Harlow, R. L.; Klooster, W. T.; Koetzle, T. F. *J. Am. Chem. Soc.* **1994**, *116*, 6812.

(74) Cramer, C. J.; Dulles, F. J.; Storer, J. W.; Worthington, S. E. *Chem. Phys. Lett.* **1994**, *218*, 387.

(75) Cramer, C. J.; Dulles, F. J.; Falvey, D. E. *J. Am. Chem. Soc.* **1994**, *116*, 9787.

(76) Cramer, C. J.; Worthington, S. E. *J. Phys. Chem.* **1995**, *99*, 1462.

(77) Matzinger, S.; Bally, T.; Patterson, E. V.; McMahon, R. J. *J. Am. Chem. Soc.* **1996**, *118*, 1535.

(78) Nash, J. J.; Squires, R. R. *J. Am. Chem. Soc.* **1996**, *118*, 11872.

(79) Smith, B. A.; Cramer, C. J. *J. Am. Chem. Soc.* **1996**, *118*, 5490.

(80) Schreiner, P. R.; Karney, W. L.; Schleyer, P. v. R.; Borden, W. T.; Hamilton, T. P.; Schaefer, H. F., III *J. Org. Chem.* **1996**, *61*, 7030.

(81) Worthington, S. E.; Cramer, C. J. *J. Phys. Org. Chem.* **1997**, *10*, 755.

(82) Bettinger, H. F.; Schreiner, P. R.; Schleyer, P. v. R.; Schaefer, H. F., III *J. Phys. Chem.* **1996**, *100*, 16147.

(83) Xie, Y. M.; Schreiner, P. R.; Schleyer, P. v. R.; Schaefer, H. F. *J. Am. Chem. Soc.* **1997**, *119*, 1370.

(84) Cramer, C. J.; Falvey, D. E. *Tetrahedron Lett.* **1997**, *38*, 1515.

(85) Cramer, C. J.; Truhlar, D. G.; Falvey, D. E. *J. Am. Chem. Soc.* **1997**, *119*, 12338.

(86) Cramer, C. J.; Smith, B. A. *J. Phys. Chem.* **1996**, *100*, 9664.

(87) Miehlisch, B.; Stoll, H.; Savin, A. *Mol. Phys.* **1997**, *91*, 527.

(88) Borowski, P.; Jordan, K. D.; Nichols, J.; Nachtigall, P. *Theor. Chem. Acc.* **1998**, *99*, 135.

(89) Gräfenstein, J.; Kraka, E.; Cremer, D. *Chem. Phys. Lett.* In press.

(90) Gordon, M. S. Personal communication.

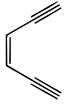

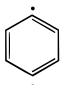
Table 2. Singlet–Triplet Splittings (H_0 , kcal/mol) of Isoelectronic Arynes^a

compd	level of theory ^b	S–T splitting
1c	BPW91 ^c	-4.0 (1.9)
	CASPT2	-5.5
	CCSD(T)	-4.9
	BCCD(T)	-4.5
	composite E ^d	-3.0
	OVBP2 ^e	-1.1
2c	BPW91	-14.0
	CASPT2	-14.1
	CCSD(T)	-12.9
	BCCD(T)	-11.6
	composite E ^d	-11.6
	OVBP2 ^e	-4.8
3c	BPW91 ^c	-4.3 (2.3)
	CASPT2	-5.6
	CCSD(T)	-29.8
	BCCD(T)	-5.6
	composite E ^d	-4.0
OVBP2 ^e	-1.3	

^a Geometries and zero-point vibrational contributions from the BPW91/cc-pVDZ level. ^b See Methods section for details on basis sets and CASPT2 active spaces. ^c Broken-symmetry unrestricted results; restricted DFT results in parentheses. ^d Equation 1. ^e Reference 29 with BPW91/cc-pVDZ ZPVE. ^f Reference 37.

To confront this problem, new developments include the exploration of hybrid combinations of MCSCF with DFT.^{87–90} As of yet, there are insufficient data to judge whether such an approach will be fruitful. Another approach, as discussed in Section 3, is to allow spin symmetry to break in the single-determinantal calculation, and to thereby permit a mixing of states that provides a more accurate description of the desired state at the expense of introducing some contamination from unwanted states of higher spin. This too is an area where more data are required prior to reaching any final conclusion with regard to the robustness of the approach. In the context of the

Table 3. Absolute (h) and Relative (kcal/mol) Energies of Bergman Cyclization Stationary Points at Different Geometries^a

level of theory ^b	geometry	 a	 b	 c(s)
CASPT2/cc-pVDZ	BPW91	-230.157 05 (0.0)	-230.120 65 (22.8)	-230.162 36 (-3.3) [-230.159 27 (-1.4)]
	CCSD(T)	-230.156 76 (0.0)	-230.119 54 (23.4)	-230.161 77 (-3.1)
CCSD(T)/cc-pVDZ	BPW91	-230.230 11 (0.0)	-230.187 42 (26.8)	-230.223 62 (4.1) [-230.219 14 (6.9)]
	CCSD(T)	-230.229 70 (0.0)	-230.185 57 (27.7)	-230.223 19 (4.1)
QCISD(T)/cc-pVDZ	BPW91	-230.231 00 (0.0)	-230.188 44 (26.7)	-230.223 76 (4.5) [-230.219 67 (7.1)]
	CCSD(T)	-230.230 57 (0.0)	-230.186 60 (27.6)	-230.223 20 (4.6)
composite E ^c	BPW91	-230.431 80 (0.0)	-230.385 75 (28.9)	-230.415 34 (10.3) [-230.412 55 (12.1)]
	CCSD(T)	-230.433 54 (0.0)	-230.384 18 (31.0)	-230.416 18 (10.9)
CCSD(T)/6-31G** ^d	CCSD(T)	-230.228 41 (0.0)	-230.182 01 (29.1)	-230.220 34 (5.1)

^a Geometries from the BPW91/cc-pVDZ (for *p*-benzynes, restricted DFT geometry results are in brackets) and CCSD(T)/6-31G** levels. ^b See Methods section for details on basis sets and CCSD(T) extrapolation. ^c Equation 1. ^d References 15 and 55.

present systems, Table 1 indicates that although the BS-UDFT thermochemistry does not agree especially well with other levels of theory, the BS-UDFT geometries of **s1c** and **s3c** are lower in energy than the restricted DFT geometries *at every level of theory*. For **s1c**, there is moreover better agreement with the CCSD(T) geometries of Kraka and Cremer for the BS-UDFT geometries than for the restricted DFT geometries. To further explore the issue of using the best possible geometries, I have carried out calculations for **1a**, **1b**, and **s1c** at all levels of theory for all three geometries (CCSD(T), restricted DFT, and BS-UDFT for **s1c**), and those results are listed in Table 3. In almost every instance, the energy of the DFT structure (BS-UDFT for **s1c**) is lower than that of the CCSD(T) structure; the only exceptions are the composite E energies for **1a** and **1c**, which are lower for the CCSD(T) structures by 0.3 and 0.5 kcal, respectively. Insofar as the DFT optimizations are *much* more economical than the CCSD(T) ones, and given the problems associated with CCSD(T) that are discussed below, it appears that this level of theory is an excellent choice for future studies on related systems (a similar conclusion has been reached by Schreiner^{22,25} and Chen et al.,²³ both of these authors have emphasized that current hybrid HF-DFT methods are to be avoided in these systems, a piece of advice I would echo strongly based on our experience with carbenes and related systems⁹¹). In the case of the six isomeric pyridynes, we have also found DFT structures to be in general lower in energy at various levels of theory compared to CAS(8,8) or CAS(10,9) structures,²⁴ a comparison that is not too surprising insofar as the latter level of theory includes no accounting for dynamic correlation. It will be interesting to compare to CASPT2 geometries once analytic gradients for that level of theory become available.

A separate issue that proves particularly problematic in the case of **s3c** is the performance of post-Hartree-Fock methods that make use of the single-determinant HF wave function as a reference, e.g., CCSD(T). Because of the high degree of multireference character in the arynes, the weight of the HF reference in the correlated wave function can become unacceptably low. Even without inspecting the wave function, it is obvious from Table 1 that something pathological occurs with **s3c**: the energy change on going from the restricted DFT geometry to the BS-UDFT geometry is -20.3 kcal! Based on the rather small differences between these two geometries,

such a difference is clearly an artifact, and a more reliable estimate of -1.9 kcal may be taken from the CASPT2 level, which accounts for the nondynamical correlation by virtue of a CAS(8,8) reference (note that the energy drop calculated with DFT is primarily associated with the change to broken symmetry; the BS-UDFT energy associated with *geometric change* is about the same as that found with CASPT2). The difficulty lies in the inadequacy of the HF wave function as the CCSD reference. In the case of the BS-UDFT geometry for **s3c**, the largest T1 and T2 amplitudes in the CCSD wave function are 0.483 and 0.485, respectively. The overlap of the left-hand CCSD wave function with the HF reference, $\langle \Psi_{\text{CCSD}} | \Psi_{\text{HF}} \rangle$, is only 0.277 (for comparison, ozone, often acknowledged as a difficult molecule based on its multireference character, has an overlap of about 0.7 to 0.8)⁹² For the restricted DFT geometry, this overlap is 0.436, and the large difference in overlap for the two geometries probably accounts for some of the instability in the energy. Such large amplitudes are in principle not a problem for CCSD, because that method involves robust infinite order summations (and indeed, there is no calculated energy difference between the two geometries at simply the CCSD level), but they are inconsistent with the fundamental assumptions of the (T) method⁹³ for perturbatively estimating the effects of triple excitations.⁹⁴ Unfortunately, it is well-known that failure to include the effects of triple excitations leads to extremely unreliable results in these aryne systems.^{15,18,20}

A curious point here is that CCSD(T) seems to deliver reliable results for **s1c**. Large energetic effects are not observed when the geometry is relaxed from restricted DFT to BS-UDFT, and the endothermicity of the Bergman reaction is, after including contributions from larger basis set calculations, in reasonable agreement with experiment. [It is worth digressing here to note that Kraka and Cremer calculated an endothermicity of 8.0 kcal, in near quantitative agreement with experiment, at the CCSD(T)/6-31G** level. However, that number requires some interpretation. It includes a differential thermal contribution of 2.5 kcal based on MP2/6-31G** frequencies. The MP2 level would be expected to be very bad indeed for *p*-benzynes (although at the time it was the best level practically available), and this may explain why at the DFT level I compute the differential thermal contribution to be only 0.7 kcal. When the

(91) This is not to say that the formalism of hybrid HF-DFT functionals is *intrinsically* flawed, but rather that present implementations of this level of theory, perhaps because HF character decreases the quality of the Kohn-Sham orbitals, are contraindicated in these systems.

(92) Stanton, J. Personal communication.

(93) Pople, J. A.; Head-Gordon, M.; Raghavachari, K. *J. Chem. Phys.* **1987**, *87*, 5968.

(94) Stanton, J. F. *Chem. Phys. Lett.* **1997**, *281*, 130.

latter value is employed, I compute⁵⁵ the CCSD(T)/6-31G** endothermicity to be 5.8 kcal. This is in fairly close agreement with the CCSD(T)/cc-pVDZ value of 4.8 kcal for the identical geometries, as would be expected given the overall similar qualities of the two basis sets employed.] The utility of CCSD(T) for *p*-benzynes is surprising because T2 cluster amplitudes similar in size to those for **s3c** are observed for the CCSD wave functions of **s1c**: At the BS-UDFT geometry, the largest T2 amplitude in the CCSD wave function is 0.393 and the overlap of the left-hand CCSD wave function with the HF reference, $\langle \Psi_{\text{CCSD}} | \Psi_{\text{HF}} \rangle$, is just 0.520.⁹² The saving grace, in this instance, probably derives from the much higher symmetry of **s1c** (D_{2h}) compared to **s3c** (C_s). In the case of **s1c**, single excitations from the b_{1u} RHF-HOMO to the a_g RHF-LUMO do not contribute to the 1A_g ground state, but in the case of **s3c**, both orbitals have a' symmetry, so single and double excitations both contribute to the $^1A'$ ground state, and indeed the former enter the CCSD wave function with large amplitude. Put somewhat differently, the high symmetry of **s1c** does not allow the RHF wave function to overlocalize in an unphysical fashion, but no such constraints are operative in the case of **s3c**.⁹² This appears to reduce the instability in the calculated triples contribution.

This observation suggests that the CCSD(T) level of theory should be applied only with caution to arynes having high degrees of multireference character but low symmetry. It also suggests a modification to the CCSD(T) formalism that might salvage the approach for low-symmetry systems, namely the use of Brueckner orbitals⁹⁵ instead of RHF orbitals in the reference wave function. Brueckner orbitals are determined self-consistently so as to eliminate contributions of single excitations to the overall wave function.^{48,96–99} Pleasantly enough, this modification seems quite efficacious—Table 1 indicates the BCCD(T) difference in energy between the two DFT geometries for **s3c** to be only 3.1 kcal, and correcting this number with larger basis set calculations reduces the difference to 2.0 kcal, in excellent agreement with the CASPT2 results. Moreover, the BCCD(T) computed singlet–triplet splitting for **3** is within 1 kcal of that predicted for **1**, an intuitively reasonable result given the isoelectronic nature of these systems. Finally, I note that when CCSD(T) instability is *not* a problem, as is the case for most of the molecules discussed in this work, the BCCD(T) results agree with the CCSD(T) results to within 1 kcal (and very often to within 0.1 kcal). It appears, then, that BCCD(T) calculations may be expected to be of considerable utility in further investigations of low-symmetry arynes where the CCSD(T) method would not be appropriate.¹⁰⁰

I now proceed to an analysis of the chemical implications of

(95) Brueckner, K. A. *Phys. Rev.* **1954**, *96*, 508.

(96) Nesbet, R. K. *Phys. Rev.* **1958**, *109*, 1632.

(97) Scuseria, G. E.; Schaefer, H. F., III *Chem. Phys. Lett.* **1987**, *142*, 354.

(98) Kobayashi, R.; Koch, H.; Jørgensen, P.; Lee, T. J. *Chem. Phys. Lett.* **1993**, *211*, 94.

(99) Scuseria, G. E. *Chem. Phys. Lett.* **1994**, *226*, 251.

(100) I have also surveyed the QCISD(T) method (Pople, J. A.; Head-Gordon, M.; Raghavachari, K. *J. Chem. Phys.* **1987**, *87*, 5968) for these systems. It appears to be much less unstable than CCSD(T), giving relative energies within 1 kcal/mol of the BCCD(T) results. This is somewhat surprising, since the single excitation amplitudes in the QCISD(T) calculations are even larger than those for the CCSD(T) calculations. Given this potential for instability, and given other criticisms of QCISD(T) theory relative to CCSD(T) or BCCD(T) (Scuseria, G. E.; Schaefer, H. F., III *J. Chem. Phys.* **1989**, *90*, 3700; Raghavachari, K.; Trucks, G. W.; Pople, J. A.; Head-Gordon, M. *Chem. Phys. Lett.* **1989**, *157*, 479; Lee, T. J.; Rendell, A. P.; Taylor, P. R. *J. Phys. Chem.* **1990**, *94*, 5463; He, Z.; Cremer, D. *Theor. Chim. Acta* **1993**, *85*, 305), I consider BCCD(T) to be the best choice in low-symmetry arynes systems where large single excitation amplitudes are observed with HF orbitals. However, further studies germane to this point are warranted.

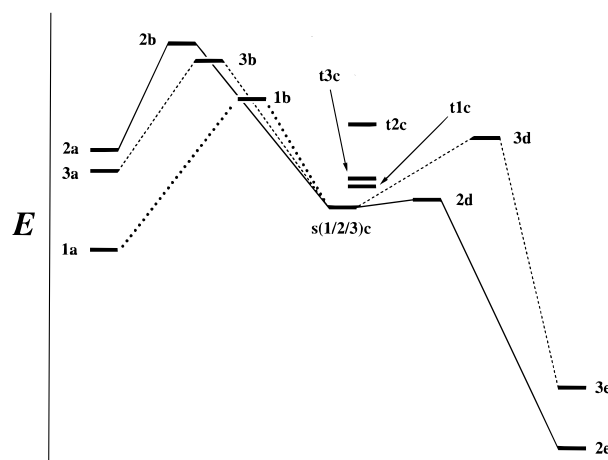


Figure 4. Overlaid reaction energetics (relative H_{298} to scale) for **1** (dotted line), **2** (solid line), and **3** (dashed line) with singlet arynes in each case taken to be the relative zero of energy. Position along the abscissa is arbitrary. Triplet arynes are also shown.

the calculations. For ease of discussion, all energies will be taken to be composite E values unless otherwise noted; on the basis of the results in Table 1 for **1**, this level of theory treats the different electron correlation effects in different isomeric structures most accurately. The CASPT2 method has been shown elsewhere to be useful for analyzing the Bergman cyclization of **1** when the method's differential accounting of correlation effects is corrected for using isodesmic reactions.¹⁸ However, the necessary heats of formation for the analogous isodesmic reactions for **2** and **3** are not available. In the absence of such corrections, the CASPT2 level of theory seriously overestimates the stability of arynes relative to enedynes and correspondingly underestimates the barrier heights for Bergman cyclizations. The OVBPT2 level employed by Hoffner et al.,²⁹ with an active space that did not include the aromatic π electrons, also predicts arynes to be too stable relative to enedynes by 6–10 kcal, but predicts Bergman transition state structures to be too *high* in energy relative to enedynes by 3–8 kcal.

The composite E level also provides good agreement with the experimental singlet–triplet gap for **1**; however, there is much better agreement between all presented levels of theory for arynes singlet–triplet splittings than is the case for cyclization thermochemistries. Exceptions are the OVBPT2 results of Hoffner et al.,²⁹ which always underestimate the gap, and CCSD(T) for **3**, which has already been discussed.

Bergman Reaction Coordinates. To facilitate comparison, Figure 4 overlays the three relevant reaction coordinates taking in each case the singlet arynes **c** as the relative zero of energy. Replacing an internal CH fragment with a nitrogen atom leads to a substantial change in the reaction enthalpy for Bergman cyclization, comparing **1a** \rightarrow **s1c** with **2a** \rightarrow **s2c**. This change of 16.3 kcal in computed exothermicity is predominantly associated with the significantly larger biradical stabilization energy (BSE) found for **s2c** compared to **s1c**. The BSE is the additional stabilization found in the biradical over and above the sum of any intrinsic stabilizations in the individual corresponding monoradicals,¹⁴ i.e., 2- and 3-pyridyl in this case. As has been noted elsewhere,²⁴ the free nitrogen lone pair in **s2c** interacts with the *para* diradical in a fashion that lowers the energy of zwitterionic resonance contributors available to the singlet wave function (but not to the triplet—this effect also manifests itself structurally in the very short singlet N–C(2) distance). Thus, at the CCSD(T) level, the BSE's of **s1c** and **s2c** are calculated to be –4.5 and –14.9 kcal, respec-

tively.^{18,24,101} The remaining energetic difference between **1** and **2** is presumably associated with the effect of nitrogen atom substitution on changes in intrinsic bond strengths upon passing from an enediyne to an aryne.

Protonation reduces the exothermicity of the aza-Bergman cyclization **a** → **c** by 3.9 kcal. At first glance, this seems rather a small change, since protonation should remove most of the stabilizing conjugation contributing to the large BSE of the aryne. However, it also appears that protonation removes a stabilizing hyperconjugative interaction in iminediyne **a**. On protonation of **2a** to **3a**, the C=N double bond increases in length by 0.025 Å and the C–C single bond antiperiplanar to the nitrogen lone pair decreases in length by 0.028 Å. Such geometric changes are consistent with the loss of a $n_N \rightarrow \sigma^*_{CC}$ stabilizing interaction.

Differences in intrinsic bond strengths also strongly influence the relative thermochemistries of the **c** → **e** steps in **2** and **3** compared to **1** (which by symmetry is **c** → **a**). The very strong nature of the C–N triple bond increases the exothermicity of this retro-Bergman reaction in **2** by 26.5 kcal compared to **1**. This extra exothermicity is reduced by about 8 kcal in **3**, consistent with nitriles being much weaker bases than aromatic nitrogen functionalities.

Increases in exothermicity from left to right along the reaction coordinate affect the various barrier heights in a fashion consistent with the Hammond¹⁰² postulate, i.e., increased exothermicities give rise to reduced barrier heights. Thus, for the **a** → **c** transformation, the computed heats of reaction are 11.0, –1.4, and –5.3 kcal for **1**, **3**, and **2**, respectively, and the corresponding barrier heights are 27.7, 21.6, and 19.4 kcal, respectively. Similarly, for the retro-Bergman cyclization that reveals an enynenitrile in the aza cases, the computed heats of reaction are –11.0, –28.4, and –37.5 kcal for **1**, **3**, and **2**, respectively, and the corresponding barrier heights are 16.7, 10.7, and 0.9 kcal, respectively.

Such an invocation of the Hammond postulate typically presupposes movement of the transition state toward reactants for an increasingly exothermic reaction. Structural analysis bears this out for the **a** → **c** transformation, where the forming C–C bond length is longest (earliest transition state) for the most exothermic cyclization (**2b**). It is 0.109 Å shorter in the next most exothermic cyclization (**3b**), and it is another 0.047 Å shorter in the endothermic cyclization (**1b**). A similar comparison of structures **d** is less informative because of intrinsic differences in C–C and C–N bond distances and the local effects of protonation.

An alternative measure of the position of the transition state structures might be to examine their biradical character based on their CAS wave functions. However, as noted by Kraka and Cremer,¹⁵ Lindh and Persson,¹⁶ and Schreiner²⁵ based on other criteria, there is very little biradical character even for the presumably late transition state structure **1b**; the ratio is 96:4 for the two configurations corresponding diabatically to the biradical configurations themselves present in **s1c** in a ratio of 64:36 (for additional comparison, the same ratio of configurations in **1a** is 99.5:0.5). The corresponding ratios of configurations in **2a**, **2b**, **s2c**, **2d**, and **2e** are 98:2, 97:3, 82:28 (reflecting the previously noted²⁴ low biradical character of **2c**), 95:5, and 98:2, respectively. For **3a**, **3b**, **s3c**, **3d**, and **3e**, the ratios are 98:2, 96:4, 64:36 (exactly the same as for **s1c**, consistent with the isoelectronic similarities of these systems), 88:12, and 98:2, respectively. The transition state structure with the highest

degree of biradical character is thus **3d**, consistent with this being an early transition state (and thus close to the aryne) for a strongly exothermic retro-Bergman cyclization. Transition state structure **2d** is probably even earlier, but since **s2c** has little biradical character, neither does **2d**.

Finally, the ionic nature of system **3** suggests that solvation effects may play an important role in modifying the relative energies of the various stationary points in aqueous solution (as would be found in vivo). Reaction-field calculations at the SM5.42R/BPW91/MIDI! level⁵³ were undertaken to evaluate differential electrostatic polarization effects, and the computed polarization free energies for **3a**, **3b**, **s3c**, **3d**, and **3e** were –57.0, –59.4, –59.4, –58.7, and –56.6 kcal, respectively. Combining these values with the data in Table 1 leads to relative energies in solution of 0.0, 19.2, –3.7, 7.6, and –29.4 kcal, respectively, i.e., solvation slightly favors the aryne and the transition state structures over the enediynes, but by at most 2.4 kcal.

Singlet–Triplet Splittings. As noted previously, all levels of theory, with the exception of the OVBPT2 results of Hoffner et al. and CCSD(T) in the case of low-symmetry **3c**, give fairly consistent estimates of the singlet–triplet splittings for the arynes. The composite E level, which is in good agreement with experiment for **1c**, predicts **3c** to have a very similar splitting to **1c**, which seems reasonable given the close similarity between these two systems (in addition, aqueous solvation effects are predicted to favor **s3c** over **t3c** by 0.5 kcal at the SM5.42R level). Aryne **2c**, on the other hand, is predicted to have a considerably more stable singlet, as discussed above and elsewhere.²⁴

An independent estimation of the state splittings may also be had from analysis of the computed ¹H isotropic hyperfine splittings (hfs) for the proton *para* to the radical in the phenyl, 3-pyridyl, and protonated 3-pyridyl radicals (2.07, 6.02, and 2.10 G, respectively). Although there is a paucity of experimental data available for validation, a strong correlation between such hyperfine splittings and computed singlet–triplet splittings has been established for several aryne systems with a proportionality constant of about –2 kcal mol^{–1} G^{–1}.^{19,24,101} These data predict singlet–triplet splittings of –4.1, –12.0, and –4.2 kcal for **1c**, **2c**, and **3c**, respectively, in excellent agreement with direct computation (and with experiment for **1c**).

Likely Utility for DNA Cleavage Reactions. In order for a given aryne to exhibit a high degree of DNA cleaving activity, it ideally should have a high degree of biradical character (this property correlating strongly with a small singlet–triplet splitting) and be thermochemically accessible from an enediyne precursor, and if alternative inactivating pathways exist (like retrocyclization to a different and more thermochemically stable enediyne), the barrier(s) for such processes should be sufficiently high to impart an appreciable lifetime to the intermediate aryne. Thus, although there are many more subtle aspects to managing strand-cleavage kinetics,²⁹ a worthwhile target for which to shoot from a design standpoint might be that the singlet–triplet splitting should be smaller in magnitude than any barrier expected to inactivate the substrate.

Aryne **s1c** falls within that design target (which is desirable, since natural systems make use of substituted **s1c** “warheads”), with an experimentally measured singlet–triplet splitting of –3.8 kcal³⁷ and retrocyclization barrier of 19.7³⁶ kcal (of course, in the case of **1**, such retrocyclization is not really “inactivating”, **1a** and **1c** being separated in energy by only somewhat over 8 kcal—see Figure 4). For free-base system **2**, on the other hand, the magnitude of the singlet–triplet splitting is predicted to be 11.6 kcal, which is 10.7 kcal larger than the barrier to retro-

(101) Cramer, C. J. Unpublished calculations.

(102) Hammond, G. S. *J. Am. Chem. Soc.* **1955**, *77*, 334.

Bergman cyclization that creates an enynenitrile that is thermodynamically more stable by 37.5 kcal. It is clearly not surprising that neither David and Kerwin³³ nor Hoffner et al.²⁹ have observed any hydrogen abstraction reactivity in related systems. Protonation of **2** delivers **3**, which shows properties intermediate between **1** and **2**: the singlet–triplet splitting is predicted to be roughly the same for **3** as for **1**, but the barrier to retro-Bergman cyclization (and in **3** such retrocyclization *would* be expected to be inactivating given its much larger exothermicity) is predicted to be reduced to 10.7 kcal. The predicted dichotomy of reactivity for **2** vs **3** is exciting to the extent it bolsters the possibility of designing pH-dependent antitumor agents.²⁹

5. Conclusions

Density functional calculations (using broken-spin-symmetry for arynes exhibiting substantial biradical character) provide very good geometries for stationary points along Bergman and aza-Bergman cyclization reaction coordinates—as good as or better than much more expensive CCSD(T) geometries. Although the CCSD(T) level of theory generally gives good results for the relative energies of (aza-)Bergman cyclization stationary points, it can fail for systems showing high degrees of biradical character where large-amplitude contributions from single excitations can occur (typically such systems will have low symmetry). Employing Brueckner orbitals remedies this instability, and BCCD(T) calculations provide good agreement with experiment for the energetics of the Bergman cyclization of **1** and for the singlet–triplet splitting of *p*-benzyne.

Such calculations predict that replacement of a CH fragment by N increases the stability of the aryne relative to the iminediyne, and drastically increases the stability of the isomeric enynenitrile. A very low barrier of 0.9 kcal for the retro-aza-Bergman cyclization of 2,5-pyridyne to enynenitrile is predicted—when combined with a predicted singlet–triplet splitting in this system of –11.6 kcal, this suggests that 2,5-pyridynes will not serve well as hydrogen atom abstracting agents. Protonation of nitrogen, on the other hand, creates a reaction coordinate intermediate between the all-carbon and unprotonated cases (both in the gas phase and aqueous solution). A low singlet–triplet splitting and moderate barrier to retro-aza-Bergman cyclization suggest that protonated 2,5-pyridynes should show reactivities similar to their all-carbon analogues.

Acknowledgment. I benefited enormously from discussions with Professor John Stanton, and am also grateful to Professors Dieter Cremer, Peter Schreiner, and Robert Squires for helpful commentary. This work was supported in part by the National Science Foundation and the Alfred P. Sloan foundation.

Supporting Information Available: Cartesian coordinates (Å) for all structures at BPW91/cc-pVDZ level (5 pages, print/PDF). See any current masthead page for ordering and Internet access instructions.

JA9806579